DALTON

Symmetrically- and asymmetrically-substituted oxo-bridged binuclear molybdenum nitrosyls: synthetic, electrochemical, spectroscopic and structural studies

Andrzej Wlodarczyk,*,†,[a] Simon J. Coles,[b] Michael B. Hursthouse,[b] K. M. Abdul Malik[b] and Harvey F. Lieberman[b]

[a] *Institute of Chemical Engineering and Physical Chemistry, Technical University of Krakow, 31-155, Krakow, Poland*
[b] *Department of Chemistry and Applied Chemistry, University of Wales Cardiff, PO Box 912, Park Place, Cardiff, UK CF1 3TB*

The binuclear μ-oxo compounds [X{HB(dmpz)$_3$}(NO)MoOMo(NO){HB(dmpz)$_3$}Y] (dmpz = 3,5-dimethylpyrazol-1-yl; X = Y = OH, OMe, OEt, OCOMe or OCOPh; X = I, Y = OH, OMe, NHMe or NHEt) have been prepared, some of these occurring as two geometric isomers (X = I, Y = OH, NHMe or NHEt) which have been separated and characterised spectroscopically. The compounds where X = Y = OH, OCOPh or OMe, and X = I, Y = OH or NHMe undergo one one-electron reduction and one one-electron oxidation, established by cyclic voltammetry, the E_f values being dependent on the donor atom of X and Y. The species where X = OCOPh undergoes an irreversible second reduction and there is an indication of very strong interaction between the metal-containing redox centres. The EPR spectrum of the mixed-valence species [(PhOCO){HB(dmpz)$_3$}(NO)-MoOMo(NO){HB(dmpz)$_3$}(OCOPh)]$^-$ ($S = \frac{1}{2}$) suggests that it is probably valence-trapped at room temperature. Some of the asymmetrically-substituted species are isolated as two isomers. A single-crystal X-ray diffraction study of [$C_{30.9}H_{47.34}B_2I_{1.16}Mo_2N_{14.90}O_3$]·0.3($C_2H_6NH$), obtained in making [I{HB(dmpz)$_3$}(NO)MoOMo(NO)-{HB(dmpz)$_3$}(NMe_2)], shows that it could contain up to four molecules, the first being the main component (*ca.* 90%): [I{HB(dmpz)$_3$(NO)MoOMo(NO){HB(dmpz)$_3$}(NHMe)], [{Mo(NO)[HB(dmpz)$_3$]I}$_2$O], [I{HB(dmpz)$_2$(4-I-dmpz)}(NO)MoOMo(NO){HB(dmpz)$_3$}(NHMe)], and perhaps [I{HB(dmpz)$_2$(4-I-dmpz)}(NO)MoOMo(NO)-{HB(dmpz)$_3$}I]. The first compound, which has *S*–*S* (or *R*–*R*) configuration at the metal centres, exhibits a slight asymmetry in the Mo–O–Mo bond system, the Mo–O–Mo bond angle being slightly bent. A geometric isomer of this compound has been isolated and characterised spectroscopically. The second compound is the enantiomer identical to the previously described [{Mo(NO)[HB(dmpz)$_3$]I}$_2$O], and the third has an iodine atom at position 4 of one of the pyrazolyl rings. Analysis, using molecular modelling calculations, of the possible isomers of these μ-oxo-bridged species with respect to rotation about a linking Mo–O bond revealed only two significantly stable forms in which one NO and an I atom on adjacent metals are mutually *cis*, and the other pair are mutually *trans*. The methylamide [I{HB(dmpz)$_3$}(NO)MoOMo(NO){HB(dmpz)$_3$}{NHMe)] adopts one of these apparently preferentially, whereas [{Mo(NO)[HB(dmpz)$_3$]I}$_2$O] can exist in two forms which have near-equivalent stability and which have been isolated and characterised previously.

In a previous paper,[1] we described the rational synthesis of the symmetrically-substituted binuclear μ-oxo chloride and iodide complexes, [{Mo(NO)[HB(dmpz)$_3$]X}$_2$O] (dmpz = 3,5-dimethylpyrazol-1-yl, X = Cl or I), and suggested mechanisms whereby these species might be formed. During our investigation of these species, we obtained the asymmetrically-substituted compounds [I{HB(dmpz)$_3$}(NO)MoOMo-{HB(dmpz)$_3$}(NO)Y] (Y = Cl or OH).[1,2] We believe that these compounds arise by reaction between species such as [Mo(NO){HB(dmpz)$_3$}I(OH)] and [Mo(NO){HB(dmpz)$_3$}Y_2] and are formed adventitiously. A more logical synthesis of such asymmetrically-substituted compounds could provide useful precursors in the construction of oligomeric redox-active compounds based on the {(ON)MoOMo(NO)}$^{2+}$ unit.

The most appropriate precursor in such a designed synthetic strategy is [{Mo(NO)[HB(dmpz)$_3$]I}$_2$O] which is a very sterically crowded molecule and which exists as two enantiomers (Fig. 1),[1,3] one of which is formed preferentially and which does not appear to convert to the other in solution. The possibility that other enantiomers might exist cannot be ruled out, as mentioned in our previous paper,[1] but most of them can be discounted on steric grounds, largely because of interactions between the methyl groups of adjacent HB(dmpz)$_3$ ligands. In exploring the potential for substitution of iodide in this sterically crowded bimetallic, two issues arise: (*a*) can substitution of I in enantiomer **B** of [{Mo(NO)[HB(dmpz)$_3$]I}$_2$O] readily occur in a stepwise fashion, (*b*) on mono-substitution, is the structural relationship between product and precursor preserved, or are other enantiomers and/or isomers formed? It is relatively easy to resolve the former, but not so simple to determine the latter since the mechanism of substitution is not

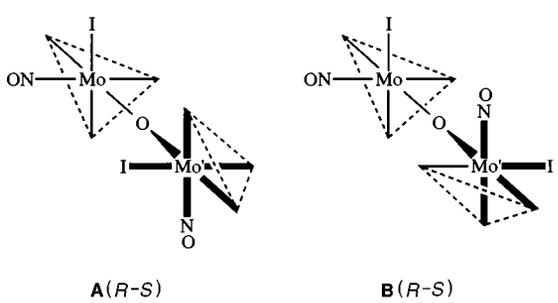

Fig. 1 Idealised structures of the structurally characterised enantiomers of [{Mo(NO)[HB(dmpz)$_3$]I}$_2$(μ-O)], **A** and **B**

† E-Mail: awlodar@usk.pk.edu.pl

known. Most transition-metal nitrosyls undergo substitution by an associative pathway because of the ability of the nitrosyl group to notionally absorb an electron pair *via* bending of the M–N–O bond, thereby releasing an acceptor orbital at the metal centre.[4] However, in these very sterically crowded binuclear species, it seems more likely that dissociation of I^- would occur, and incorporation of the incoming nucleophile could occur with loss of configuration at the metal centre. We currently have no information which illuminates this point. It is also possible that enantiomer interconversion might occur during substitution as a result of rotation about the Mo–O–Mo bond system, although this seems very unlikely from construction of simple space-filling models.

In this paper, we describe substitution reactions of [{Mo(NO)[HB(dmpz)$_3$]I}$_2$O], the formation of mono- and di-substituted species, their spectroscopic and, where appropriate, electrochemical characterisation, and an X-ray structural characterisation of an isomer of the mono-substituted species [I{HB(dmpz)$_3$}(NO)MoOMo(NO){HB(dmpz)$_3$}(NHMe)].

Experimental

All reagents were used as purchased without further purification except [{Mo(NO)[HB(dmpz)$_3$]I}$_2$O] which was prepared as described earlier.[1] Solvents were specially purified, dried and degassed as discussed previously,[1] and all yields are based on the starting metal-containing compound.

Proton NMR spectra were recorded on a JEOL GX270 instrument, some fast atom bombardment (FAB) mass spectra were obtained using a VG-Autospec of the SERC Mass Spectrometry Service Centre, Swansea, and others using a similar instrument in the School of Chemistry in Bristol, with 3-nitrobenzyl alcohol as matrix. Infrared spectra were measured in KBr discs using a PE1600 Fourier-transform IR spectrophotometer. Microanalyses were determined by the Microanalytical Laboratory of the School of Chemistry, University of Bristol. Electrochemical measurements were made using an EG & PAR model 273A potentiostat. Dichloromethane, purified by distillation from CaH_2, was used as solvent and [NBu$^n_4$][PF$_6$] (0.1 M) as base electrolyte. A standard three-electrode configuration was used, with Pt-bead working and auxiliary electrodes, and a saturated calomel electrode (SCE) as reference. Ferrocene was added at the end of each experiment as an internal standard; all potentials are quoted *vs*. the ferrocene–ferrocenium couple ($Fc–Fc^+$).

Synthetic studies

[{Mo(NO)[HB(dmpz)$_3$](OCOMe)}$_2$(μ-O)] 1. To a solution of [{Mo(NO)[HB(dmpz)$_3$]I}$_2$(μ-O)] (0.2 g, 1.8 mmol) in toluene (50 cm^3), which had been refluxed for 0.5 h, was added AgOCOMe (0.5 g). The mixture was stirred and refluxed for 1 h affording a magenta solution. Petroleum ether (b.p. 40–60°) or *n*-hexane was added to precipitate inorganic salts, and the reaction mixture was then filtered. The filtrate was evaporated *in vacuo*, the residue recrystallised from acetone–*n*-hexane to afford the complex as dark brown microcrystals (0.08 g, 44%) (Found: C, 41.9; H, 5.3; N, 19.0. $C_{34}H_{50}B_2Mo_2N_{14}O_7$ requires C, 41.7; H, 5.1; N, 20.0%); *M* (FAB mass spectrum) 981 (calc. 980.4); ν_{max} 1698 (NO), 1660 (NO), 769 cm^{-1} (MoOMo); δ_H(CDCl$_3$) 5.98, 5.82, 5.80, 5.51, 5.30 (1 H, s; 2 H, s; 1 H, s; 1 H, s; 1 H, s; Me$_2$C$_3$*H*N$_2$); 2.86, 2.57, 2.47, 2.39, 2.38, 2.31, 1.03, 0.73 [3 H, s; 3 H, s; 3 H, s; 3 H, s; 6 H, s; 6 H, s; 3 H, s; 3 H, s; (C*H*$_3$)$_2$C$_3$HN$_2$]; 2.18, 2.19 (3 H, s; 3 H, s; OCOC*H*$_3$).

[{Mo(NO)[HB(dmpz)$_3$](OCOPh)}$_2$(μ-O)] 2. This compound was prepared in the same way as the acetate above using AgOCOPh, the reaction taking place over 3 h. The crude product was purified by column chromatography on silica gel using dichloromethane to elute the first fraction, identified as [{Mo(NO)[HB(dmpz)$_3$]I}$_2$(μ-O)], and a mixture of tetrahydrofuran (thf) (10% v/v)–dichloromethane to elute the product as the main fraction. The solvent was evaporated *in vacuo* and the residue recrystallised from acetone–*n*-hexane affording the product as brown microcrystals (0.07 g, 35%) (Found: C, 48.8; H, 4.9; N, 17.3. $C_{42}H_{54}B_2Mo_2N_{14}O_7$ requires C, 48.1; H, 4.5; N, 17.8%); *M* (FAB mass spectrum) 1106 (calc. 1099.5); ν_{max} 1708 (NO), 1660 (NO), 759 cm^{-1} (MoOMo); δ_H 8.00, 7.73, 7.47–7.23 (2 H, m; 2 H, m; 6 H, m; OCOC$_6$H$_5$); 6.05, 5.74, 5.54, 5.46, 5.33 (1 H, s; 2 H, s; 1 H, s; 1 H, s; 1 H, s; Me$_2$C$_3$*H*N$_2$); 3.15, 2.48, 2.42, 2.40, 2.36, 2.33, 2.31, 2.30, 2.26, 2.20, 1.12, 0.69 [3 H, s; 3 H, s; 3 H, s; 3 H, s; 3 H, s; 3 H, s; 3 H, s; 3 H, s; 3 H, s; 3 H, s; 3 H, s; 3 H, s; (C*H*$_3$)$_2$C$_3$HN$_2$].

[{Mo(NO)[HB(dmpz)$_3$](OH)}$_2$(μ-O)] 3. A mixture of [{Mo(NO)[HB(dmpz)$_3$](OCOMe)}$_2$(μ-O)] **1** (0.05 g, 0.05 mmol) and water (0.2 cm^3) in toluene (30 cm^3) was stirred and refluxed for 5 h. The solution was then cooled, evaporated *in vacuo* and the solid residue dissolved in the minimum volume of dichloromethane. Purification was effected by column chromatography on silica gel, using thf (2% v/v)–dichloromethane as eluent. The main red fraction was collected, the solvent evaporated *in vacuo* and the product recrystallised from dichloromethane–*n*-hexane, being isolated as pink crystals (0.02 g, 49%). The compound could also be obtained, in *ca*. 20% yield, by the reaction of [{Mo(NO)[HB(dmpz)$_3$]I}$_2$(μ-O)] with a 40% aqueous solution of NH_2Me in toluene (20 h under reflux) (Found: C, 40.5; H, 5.7; N, 20.7. $C_{30}H_{46}B_2Mo_2N_{14}O_5$ requires C, 40.2; H, 5.2; N, 21.9%); *M* (FAB mass spectrum) 896 (calc. 1006.2); ν_{max} 1654 (NO), 1627 (NO), 776 cm^{-1} (MoOMo); δ_H(CDCl$_3$) 5.99, 5.80, 5.78, 5.50, 5.33 (1 H, s; 2 H, s; 1 H, s; 1 H, s; 1 H, s; Me$_2$C$_3$*H*N$_2$); 2.94, 2.77, 2.48, 2.38, 2.38, 2.35, 2.33, 2.29, 2.28, 1.02, 0.81 [3 H, s; 3 H, s; 3 H, s; 3 H, s; 3 H, s; 6 H, s; 3 H, s; 3 H, s; 3 H, s; 3 H, s; 3 H, s; (C*H*$_3$)$_2$C$_3$HN$_2$].

[I{HB(dmpz)$_3$}(NO)MoOMo(NO){HB(dmpz)$_3$}(OH)] 4. A mixture of [{Mo(NO)[HB(dmpz)$_3$]I}$_2$(μ-O)] (0.11 g, 0.1 mmol), an excess of AgOCOMe and water (0.2 cm^3) was stirred and refluxed in toluene (30 cm^3) for 3 h. The mixture was filtered, the filtrate evaporated *in vacuo*, and the residue chromatographed on silica gel. Using thf (2% v/v)–dichloromethane as eluent, two pink fractions were separated and collected. After evaporation of the solvent, the products were recrystallised from dichloromethane–*n*-hexane, affording two isomers/rotamers of the product as pink microcrystals (isomer **4a**, 0.03 g, 29%; isomer **4b**, 0.02 g, 19%). Isomer **4a** (Found: C, 36.6; H, 4.6; N, 18.8. $C_{30}H_{45}B_2IMo_2N_{14}O_4$ requires C, 35.8; H, 4.5; N, 19.5%); *M* (FAB mass spectrum) 1007 (calc. 1006.2); ν_{max} 1676 (NO), 1650 (NO), 763 cm^{-1} (MoOMo); δ_H(CDCl$_3$) 9.36 (1 H, m, OH); 6.05, 5.90, 5.80, 5.79, 5.48, 5.33 (1 H, s; 1 H, s; 1 H, s; 1 H, s; 1 H, s; Me$_2$C$_3$*H*N$_2$); 3.15, 3.04, 2.52, 2.43, 2.40, 2.39, 2.34, 2.33, 2.30, 2.29, 0.94, 0.80 [3 H, s; 3 H, s; 3 H, s; 3 H, s; 3 H, s; 3 H, s; 3 H, s; 3 H, s; 3 H, s; 3 H, s; 3 H, s; (C*H*$_3$)$_2$C$_3$HN$_2$]. Isomer **4b** (Found: C, 37.7; H, 4.7; N, 19.0. $C_{30}H_{45}B_2IMo_{12}N_{14}O_4$ requires C, 35.8; H, 4.5; N, 19.5%); *M* (FAB mass spectrum) 1007 (calc. 1006.2); ν_{max} 1671 (NO), 1645 (NO), 758 cm^{-1} (MoOMo); δ_H(CDCl$_3$) 9.40 (1 H, s, OH); 5.93, 5.82, 5.80, 5.76, 5.61, 5.46 (1 H, s; 1 H, s; 1 H, s; 1 H, s; 1 H, s; Me$_2$C$_3$*H*N$_2$); 2.85, 2.56, 2.41, 2.38, 2.36, 2.34, 2.29, 2.27, 1.03, 0.98 [6 H, s; 3 H, s; 6 H, s; 3 H, s; 3 H, s; 3 H, s; 3 H, s; 3 H, s; 3 H, s; 3 H, s; (C*H*$_3$)$_2$C$_3$HN$_2$].

[I{HB(dmpz)$_3$}(NO)MoOMo(NO){HB(dmpz)$_3$}(OMe)] 5. A mixture of [{Mo(NO)[HB(dmpz)$_3$]I}$_2$(μ-O)] (0.11 g, 0.1 mmol), methanol (0.5 cm^3) and AgOCOMe (0.3 g) in toluene (50 cm^3) was stirred and refluxed for 3 h. The mixture was cooled, filtered and the filtrate evaporated *in vacuo*. The residue was chromatographed as above using dichloromethane as eluent, a main pink fraction being separated and collected. After evapor-

ation of the solvent, the residue was recrystallised from dichloromethane–*n*-hexane affording the product as pink microcrystals (0.04 g, 37%) (Found: C, 36.8; H, 4.8; N, 18.7. $C_{31}H_{47}B_2IMo_2N_{14}O_4$ requires C, 36.5; H, 4.6; N, 19.2%); *M* (FAB mass spectrum) 1921 (calc. 1020.2); ν_{max} 1670 (NO), 1650 (NO), 750 cm^{-1} (MoOMo); $\delta_H(CDCl_3)$ 5.99, 5.84, 5.83, 5.80, 5.50, 5.37 (1 H, s; 1 H, s; 1 H, s; 1 H, s; 1 H, s; 1 H, s; $Me_2C_3HN_2$); 5.04 (3 H, s; OCH_3); 3.01, 2.87, 2.55, 2.49, 2.36, 2.36, 2.33, 2.30, 0.95, 0.74 [3 H, s; 3 H, s; 3 H, s; 3 H, s; 6 H, s; 3 H, s; 3 H, s; 6 H, s; 3 H, s; 3 H, s; $(CH_3)_2C_3HN_2$].

[{Mo(NO)[HB(dmpz)$_3$](OMe)}$_2$(μ-O)] 6. A mixture of [{Mo(NO)[HB(dmpz)$_3$]I}$_2$(μ-O)] (0.11 g, 0.1 mmol), dry methanol (40 cm^3) and AgOCOMe (0.5 g) was stirred and refluxed for 3 h. The mixture was cooled, filtered and the filtrate evaporated *in vacuo*. Separation and purification of the product was as described above, the compound being recrystallised from dichloromethane–*n*-hexane and isolated as pink microcrystals (0.05 g, 51%) (Found: C, 42.6; H, 5.6; N, 20.3. $C_{32}H_{50}B_2Mo_2N_{14}O_5$ requires C, 41.6; H, 5.5; N, 21.2%); *M* (FAB mass spectrum) 925 (calc. 924.3); ν_{max} 1639 (NO), 1619 (NO), 762 cm^{-1} (MoOMo); $\delta_H(CDCl_3)$ 5.93, 5.82, 5.79, 5.75, 5.41, 5.27 (1 H, s; 1 H, s; 1 H, s; 1 H, s; 1 H, s; 1 H, s; $Me_2C_3HN_2$); 5.18, 4.83 (3 H, s; 3 H, s; OCH_3); 2.92, 2.60, 2.58, 2.49, 2.36, 2.34, 2.33, 2.29, 2.28, 0.99, 0.72 [3 H, s; 3 H, s; 3 H, s; 3 H, s; 3 H, s; 3 H, s; 6 H, s; 3 H, s; 3 H, s; 3 H, s; 3 H, s; $(CH_3)_2C_3HN_2$].

[{Mo(NO)[HB(dmpz)$_3$](OEt)}$_2$(μ-O)] 7. The complex [{Mo(NO)[HB(dmpz)$_3$](OCOMe)}$_2$(μ-O)] (0.11 g, 0.1 mmol) was stirred and refluxed in absolute ethanol (40 cm^3) for 1 h. The solution was evaporated to dryness *in vacuo*, the solid residue dissolved in the minimum volume of dichloromethane, and chromatographed on silica gel using dichloromethane as initial eluent. The elutants were discarded. The main pink fraction was then separated using thf (20% v/v)–dichloromethane mixture as eluent. After collection and evaporation of the solvent, the pink product was isolated by precipitation on dropwise addition of *n*-hexane to a dichloromethane solution of the compound (0.06 g, 67%) (Found: C, 42.8; H, 5.7; N, 20.3. $C_{34}H_{54}B_2Mo_2N_{14}O_5$ requires C, 42.9; H, 5.7; N, 20.6%); *M* (FAB mass spectrum) 952 (calc. 952.2); ν_{max} 1644 (NO), 1622 (NO), 761 cm^{-1} (MoOMo); $\delta_H(CDCl_3)$ 5.92, 5.81, 5.78, 5.77, 5.40, 5.28 (1 H, s; 1 H, s; 1 H, s; 1 H, s; 1 H, s; 1 H, s; $Me_2C_3HN_2$); 5.47, 5.01 (2 H, m; 2 H, m; OCH_2Me); 2.94, 2.63, 2.60, 2.49, 2.35, 2.34, 2.29, 2.28, 0.99, 0.78 [3 H, s; 3 H, s; 3 H, s; 3 H, s; 6 H, s; 6 H, s; 3 H, s; 3 H, s; 3 H, s; 3 H, s; $(CH_3)_2C_3HN_2$]; 1.50, 1.11 (3 H, t; 3 H, t; OCH_2CH_3).

Two isomers of [I{HB(dmpz)$_3$}(NO)MoOMo(NO){HB(dmpz)$_3$}(NHMe)] 8. Gaseous NH_2Me was slowly bubbled through a solution of [{Mo(NO)[HB(dmpz)$_3$]I}$_2$(μ-O)] (0.11 g, 0.1 mmol) in thf (40 cm^3). After 3 h the dark orange solution was evaporated to dryness *in vacuo*, the residue extracted with diethyl ether, and the solution filtered. After evaporation of the solvent, purification was effected as described above, using *n*-hexane (10% v/v)–dichloromethane as eluent on silica gel. The main brown fraction, which contains two isomers/rotamers, was collected and evaporated to dryness. Partial crystallisation of the residue from dichloromethane–*n*-hexane mixtures, afforded orange crystals of **8a** (0.02 g, 20%). The mother-liquor from this recrystallisation was evaporated to dryness affording 0.04 g of the bimetallic species (43% overall yield), and was shown by ^{1}H NMR spectroscopy to be a mixture of two isomers/rotamers (**8a**, above, and **8b**) in the approximate ratio 1:2. Isomer **8a** (Found: C, 37.0; H, 5.1; N, 20.3. $C_{31}H_{48}B_2IMo_2N_{15}O_3$ requires C, 36.5; H, 4.7; N, 20.6%); *M* (FAB mass spectrum) 1020 (calc. 1019); ν_{max} 1659 (NO), 1638 (NO), 745 cm^{-1} (MoOMo); $\delta_H(CDCl_3)$ 10.54 (1 H, br, N*H*Me); 5.90, 5.83, 5.80, 5.76, 5.49, 5.41 (1 H, s; 1 H, s; 1 H, s; 1 H, s; 1 H, s; 1 H, s; $Me_2C_3HN_2$); 4.52 [3 H, d, *J*(HH) 7.7 Hz, $NHCH_3$]; 2.82, 2.74, 2.60, 2.40, 2.36, 2.36, 2.34, 2.29, 2.28, 0.99, 0.86 [3 H, s; 3 H, s; 3 H, s; 6 H, s; 3 H, s; 3 H, s; 3 H, s; 3 H, s; 3 H, s; 3 H, s; 3 H, s; 3 H, s; 3 H, s; $(CH_3)_2C_3HN_2$]. Isomer **8b**: ν_{max} 1659 (NO), 1638 (NO), 745 cm^{-1} (MoOMo); $\delta_H(CDCl_3)$ 9.55 (1 H, br, N*H*Me); 5.97, 5.83, 5.78, 5.77, 5.44, 5.37 (1 H, s; 1 H, s; 1 H, s; 1 H, s; 1 H, s; 1 H, s; $Me_2C_3HN_2$); 4.25 [3 H, d, *J*(HH) 7.5 Hz, $NHCH_3$]; 3.11, 3.01, 2.56, 2.48, 2.38, 2.36, 2.35, 2.33, 2.29, 2.28, 0.85, 0.78 [3 H, s; 3 H, s; 3 H, s; 3 H, s; 3 H, s; 3 H, s; 3 H, s; 3 H, s; 3 H, s; 3 H, s; 3 H, s; 3 H, s; $(CH_3)_2C_3HN_2$].

Two isomers of [I{HB(dmpz)$_3$}(NO)MoOMo(NO){HB(dmpz)$_3$}(NHEt)] 9. A mixture of [{Mo(NO)[HB(dmpz)$_3$]I}$_2$(μ-O)] (0.11 g, 0.1 mmol) and dry NH_2Et (0.3 cm^3) in thf (40 cm^3) was stirred and refluxed for 3 h. The resultant light brown solution was evaporated to dryness *in vacuo*, and the residue extracted with diethyl ether. The extract was evaporated and the residue redissolved in the minimum volume of dichloromethane and purified by column chromatography using *n*-hexane (10% v/v)–dichloromethane as eluent. After evaporation of the first brown fraction, the solid was recrystallised from dichloromethane–ethanol affording the product as brown crystals, **9a** (0.018 g, 17%). The main brown fraction was separated similarly, the solid being recrystallised from dichloromethane–*n*-hexane, affording light brown microcrystals of **9b** (0.04 g, 41%). Isomer **9a** (Found: C, 38.2; H, 4.9; N, 20.3. $C_{32}H_{50}B_2IMo_2N_{15}O_3$ requires C, 37.2; H, 4.9; N, 20.3%); *M* (FAB mass spectrum) 1035 (calc. 1033); ν_{max} 1659 (NO), 1640 (NO), 746 cm^{-1} (MoOMo); $\delta_H(CDCl_3)$ 10.39 (1 H, br, N*H*Et); 5.90, 5.85, 5.79, 5.75, 5.47, 5.40 (1 H, s; 1 H, s; 1 H, s; 1 H, s; 1 H, s; 1 H, s; $Me_2C_3HN_2$); 5.10, 4.67 (1 H, m; 1 H, m; $NHCH_2Me$); 2.85, 2.81, 2.60, 2.40, 2.39, 2.37, 2.35, 2.29, 2.27, 0.99, 0.87 [3 H, s; 3 H, s; 3 H, s; 3 H, s; 3 H, s; 3 H, s; 6 H, s; 3 H, s; 3 H, s; 3 H, s; 3 H, s; $(CH_3)_2C_3HN_2$]; 1.48 (3 H, t, $NHCH_2CH_3$). Isomer **9b** (Found: C, 37.6; H, 5.0; N, 20.2. $C_{32}H_{50}B_2IMo_2N_{15}O_3$ requires C, 37.2; H, 4.9; N, 20.3%); *M* (FAB mass spectrum) 1035 (calc. 1033); ν_{max} 1655 (NO), 1638 (NO), 744 cm^{-1} (MoOMo); $\delta_H(CDCl_3)$ 9.35 (1 H, br, N*H*Et); 5.96, 5.86, 5.77, 5.76, 5.45, 5.39 (1 H, s; 1 H, s; 1 H, s; 1 H, s; 1 H, s; 1 H, s; $Me_2C_3HN_2$); 4.91, 4.43 (1 H, m; 1 H, m; $NHCH_2Me$); 3.10, 3.01, 2.56, 2.48, 2.39, 2.38, 2.34, 2.29, 2.29, 0.87, 0.81 [3 H, s; 3 H, s; 3 H, s; 3 H, s; 3 H, s; 3 H, s; 6 H, s; 3 H, s; 3 H, s; 3 H, s; 3 H, s; $(CH_3)_2C_3HN_2$]; 1.11 (3 H, t, $NHCH_2CH_3$).

Crystal and molecular structure of [I(ON){HB(dmpz)$_3$}MoOMo(NO){HB(dmpz)$_3$}(NHMe)] 8a

The crystals were obtained from dichloromethane–carbon tetrachloride mixtures.

Crystal data. $C_{30.9}H_{47.34}B_2I_{1.16}Mo_2N_{14.90}O_3 \cdot 0.3(C_2H_6NH)$, $M = 1050.30$, monoclinic, space group $P2_1/n$ (alternative $P2_1/c$, no. 14), $a = 14.285(3)$, $b = 15.076(3)$, $c = 20.379(4)$ Å, $\beta = 95.19(2)°$, $U = 4371(2)$ Å^3 (by least-squares refinement of diffractometer angles for 250 reflections within $\theta = 1.82–25.09°$, $\lambda = 0.710\,69$ Å), $Z = 4$, $D_c = 1.596$ g cm^{-3}, $F(000) = 2098$, $\mu = 14.43$ cm^{-1}, $T = 150$ K, orange parallelipiped, crystal size $0.25 \times 0.18 \times 0.15$ mm.

Data collection and processing. A Delft Instruments FAST TV area detector diffractometer positioned at the window of a rotating anode generator (Mo-Kα radiation, $\lambda = 0.710\,96$ Å) was used.[5] 17 958 Reflections were measured ($\theta = 1.82–25.08°$; index ranges $-17 \leqslant h \leqslant 13$; $-16 \leqslant k \leqslant 17$; $-24 \leqslant l \leqslant 22$), 6605 unique with intensities greater than zero [merging $R = 0.0635$ after absorption correction (maximum and minimum absorption corrections factors = 0.893, 1.021)]. The structure was solved by direct methods and refined on F_o^2 by full-matrix least squares using all unique data. The structure exhibited a complicated nature of disorder. Refinement of the model without disorder resulted in a conventional *R* value of *ca*. 0.09 (on observed

data only), with significant residual electron densities in the region of the methylamido group as well as at a distance of *ca.* 2.1 Å from one atom [C(7)] of a $Me_2C_3HN_2$ group on the other Mo atom. These residuals were assumed to be associated with partially occupied iodide species. Successful refinement was achieved on the basis of a 'disordered' model with the methylamino (90%) and iodo (10%) ligands occupying the same co-ordination site around Mo(2), and with an additional iodine bonded to C(7) with a 6% occupancy of the relevant site. The difference map also contained another region of significant electron density, which was modelled on a partially occupied (30%) Me_2NH solvate (we have no other explanation for this other than the occurrence of dimethylamine as an impurity in the gaseous methylamine used in the synthesis: there is some weak evidence for this from ^{1}H NMR spectroscopy, but see Conclusion section). All non-hydrogen atoms (except those on the Me_2NH) were anisotropic. The H of the methylamino group and those on the solvate were ignored; others were included in idealised positions with U_{iso} set at 1.2 (CH) or 1.5 (CH_3) times the U_{eq} of the parent. This model, accepted as the 'correct' structure, gave final R [$=\Sigma(F_o - F_c)/\Sigma(F_o)$] and wR [$=\Sigma\{w(F_o^2 - F_c^2)^2\}/\Sigma\{w(F_o^2)^2\}]^{\frac{1}{2}}$ values of 0.1038 and 0.1530 respectively for 529 parameters and all 6605 data [ρ_{min}, ρ_{max} −1.12, 1.46 e Å^{-3}; $(\Delta/\sigma)_{max}$ 0.34]. The corresponding R values for 3367 data with $I > 2\sigma(I)$ were 0.0519 and 0.1459. Weighting scheme, $w = 1/[\sigma^2(F_o^2) + (0.0621P)^2]$, where $P = [\max(F_o)^2 + 2(F_c)^2]/3$, gave satisfactory agreement analyses. The programs used were DIFABS (absorption correction),[6] SHELXS (structure solution),[7] SHELXL 93 (refinement)[8] and SNOOPI (diagrams).[9] Calculations were performed on a 486DX2/66 personal computer; sources of scattering factor data as in ref. 8. Selected geometry parameters are given in Table 1.

CCDC reference number 186/621.

Table 1 Selected bond lengths (Å) and angles (°) for complex **8a**

Mo(1)–O(1)	1.884(6)	Mo(2)–O(1)	1.948(6)
Mo(1)–N(1)	2.224(8)	Mo(2)–N(7)	2.238(8)
Mo(1)–N(3)	2.235(9)	Mo(2)–N(9)	2.226(8)
Mo(1)–N(5)	2.156(8)	Mo(2)–N(11)	2.228(8)
Mo(1)–N(13)	1.752(9)	Mo(2)–N(14)	1.773(9)
Mo(1)–I(1)	2.768(1)	Mo(2)–I(2)*	2.666(13)
		Mo(2)–N(15)*	1.967(12)
B(1)–N(6)	1.52(2)	B(2)–N(8)	1.529(14)
B(1)–N(4)	1.56(2)	B(2)–N(12)	1.556(14)
B(1)–N(2)	1.570(14)	B(2)–N(10)	1.564(14)
O(13)–N(13)	1.207(10)	O(14)–N(14)	1.205(10)
O(1)–Mo(1)–N(1)	163.0(3)	O(1)–Mo(2)–N(7)	89.1(3)
O(1)–Mo(1)–N(3)	85.2(3)	O(1)–Mo(2)–N(9)	163.5(3)
O(1)–Mo(1)–N(5)	90.8(3)	O(1)–Mo(2)–N(11)	87.4(3)
O(1)–Mo(1)–N(13)	95.7(3)	O(1)–Mo(2)–N(14)	96.7(3)
O(1)–Mo(1)–I(1)	106.9(2)	O(1)–Mo(2)–I(2)*	105.0(3)
		O(1)–Mo(2)–N(15)*	101.9(4)
N(1)–Mo(1)–N(3)	84.1(3)	N(7)–Mo(2)–N(9)	77.3(3)
N(1)–Mo(1)–N(3)	75.5(3)	N(7)–Mo(2)–N(11)	86.7(3)
N(3)–Mo(1)–N(5)	87.3(3)	N(9)–Mo(2)–N(11)	82.6(3)
N(13)–Mo(1)–N(1)	95.4(3)	N(14)–Mo(2)–N(7)	92.7(3)
N(13)–Mo(1)–N(3)	178.4(3)	N(14)–Mo(2)–N(9)	93.3(3)
N(13)–Mo(1)–N(5)	93.9(3)	N(14)–Mo(2)–N(11)	175.8(3)
N(1)–Mo(1)–I(1)	85.7(2)	N(7)–Mo(2)–I(2)*	165.8(3)
		N(7)–Mo(2)–N(15)*	165.4(4)
N(3)–Mo(1)–I(1)	87.2(2)	N(9)–Mo(2)–I(2)*	88.6(3)
		N(9)–Mo(2)–N(15)*	90.2(5)
N(5)–Mo(1)–I(1)	160.9(2)	N(11)–Mo(2)–I(2)*	92.2(3)
		N(11)–Mo(2)–N(15)*	84.3(4)
N(13)–Mo(1)–I(1)	91.3(3)	N(14)–Mo(2)–I(2)*	87.4(4)
		N(14)–Mo(2)–N(15)*	95.5(4)
N(4)–B(1)–N(2)	108.0(9)	N(8)–B(2)–N(10)	107.0(8)
N(6)–B(1)–N(2)	108.4(9)	N(8)–B(2)–N(12)	110.2(9)
N(6)–B(1)–N(4)	110.7(9)	N(12)–B(2)–N(10)	108.7(8)
Mo(1)–O(1)–Mo(2)	167.8(4)		

* I(2) (90%) and N(15) (10%) occupy the same co-ordination site around Mo(2).

Results and Discussion

Synthesis

When [{Mo(NO)[HB(dmpz)$_3$]I}$_2$O] was treated with silver acetate under anhydrous conditions, the symmetric dark brown bis(acetate) [{Mo(NO)[HB(dmpz)$_3$](OAc)}$_2$O] **1** was obtained which is stable in the absence of water. The analogous [{Mo(NO)[HB(dmpz)$_3$](OCOPh)}$_2$O] **2** could be made similarly using silver benzoate. Water reacted with complex **1** giving the symmetric red bis(hydroxide) [{Mo(NO)[HB(dmpz)$_3$](OH)}$_2$O] **3** which we fortuitously discovered could also be made by reaction of [{Mo(NO)[HB(dmpz)$_3$]I}$_2$O] with wet $MeNH_2$ (but see below).

By refluxing [{Mo(NO)[HB(dmpz)$_3$]I}$_2$O] with silver acetate in *dry* methanol [{Mo(NO)[HB(dmpz)$_3$](OMe)}$_2$O] **6** can be produced, presumably *via* **1**, and when **1** is refluxed in absolute ethanol, the symmetrically-substituted bis(ethoxide) **7** is formed. These compounds were isolated as single enantiomers; no evidence was obtained for the existence of the other enantiomer.

Very careful treatment of [{Mo(NO)[HB(dmpz)$_3$]I}$_2$O] with AgOCOMe and water affords two isomers of the pink iodo–hydroxide [I{HB(dmpz)$_3$}(NO)MoOMo(NO){HB(dmpz)$_3$}(OH)] **4** which can be separated chromatographically. However, only one isomer of [I{HB(dmpz)$_3$}(NO)MoOMo(NO){HB(dmpz)$_3$}(OH)] is apparently produced, as a minor product, in the reaction between [Mo(CO)$_2$(NO){HB(dmpz)$_3$}], iodine and water in refluxing toluene, as described previously.[1] The related methoxide [I{HB(dmpz)$_3$}(NO)MoOMo(NO){HB(dmpz)$_3$}(OMe)] **5** is obtained using methanol instead of water, but only one isomer could be isolated in yields sufficient for characterisation.

Two orange isomers of both [I{HB(dmpz)$_3$}(NO)MoOMo(NO){HB(dmpz)$_3$}(NHMe)] **8a** and **8b**, and of [I{HB(dmpz)$_3$}(NO)MoOMo(NO){HB(dmpz)$_3$}(NHEt)] **9a** and **9b**, are formed by reacting [{Mo(NO)[HB(dmpz)$_3$]I}$_2$O] in thf with anhydrous RNH_2 (R = Me or Et). Again, the isomers can be separated satisfactorily by column chromatography.

All complexes provide reasonably satisfactory elemental analyses, and FAB mass spectral studies of the majority exhibit molecular ions.

Spectroscopic studies

The IR spectra of the binuclear compounds contain ν_{BH} in the region 2450–2495 cm^{-1} in addition to other bands attributable to the presence of the HB(dmpz)$_3$ ligand. The binuclear compounds also exhibit two NO stretching frequencies, consistent with the general structures already established for the enantiomers of [{Mo(NO)[HB(dmpz)$_3$]I}$_2$O].[1,3] The values of ν_{NO} generally reflect the electron-withdrawing or -releasing properties of the atoms or groups, X and Y, in [X{HB(dmpz)$_3$}(NO)MoOMo(NO){HB(dmpz)$_3$}Y], decreasing in the order, X, Y = I, I > I, OH > I, OMe > I, NHMe ≈ I, NHEt and X, Y = OCOPh, OCOPh ⩾ OCOMe , OCOMe ⩾ I, I > OH, OH > OEt, OEt ⩾ OMe, OMe. The differences between the values of ν_{NO} for comparable pairs of isomers/enantiomers rarely exceed 5 cm^{-1}. The asymmetric Mo–O–Mo stretching mode appears in the range 744–776 cm^{-1} and while there are no clear trends relating to the electronegativities of X and Y, generally ν_{MoOMo} is at the lower end of the range when X and/or Y is I, presumably reflecting the effect of the heavier halogen atom on the stretching force constant.

The ^{1}H NMR spectra reflect the lack of a plane, axis or centre of symmetry in these molecules. The protons attached to the C^4 atom of the pyrazolyl rings generally resonate in the range δ 6.05–5.27. However, the signals due to the methyl groups occur over a range of *ca.* 2.5 ppm (δ 3.23–0.69), which is

Table 2 Cyclic voltammetric data obtained for [X{HB(dmpz)$_3$}(ON)MoOMo(NO){HB(dmpz)$_3$}Y]

Compound			Reduction processes					Oxidation process	
X	Y	Base electrolyte	$E_f^1(\Delta E_p)$ *vs.* SCE[a]	E_f^1 *vs.* Fc[b]	$E_f^2(\Delta E_p)$ *vs.* SCE[c]	E_f^2 *vs.* Fc[b]	ΔE_f[d] ($E_f^1 - E_f^2$)	$E_f^3(\Delta E_p)$ *vs.* SCE	E_f^3 *vs.* Fc[b]
OH	OH	$[Bu_4N][PF_6]$	−0.97(365)[e]	−1.77[e]	Not observed	—		+1.40[e,f]	+0.60[e]
OMe	OMe	$[Bu_4N][PF_6]$	−1.40(250)[e]	−1.84[e]	Not observed	—	—	+1.04(60)[g]	+0.59
OCOPh	OCOPh	$[Bu_4N][PF_6]$	−0.79(86)	−1.24	−2.03[h]	−2.48[h]	(1240)[i]	+1.36[h]	+0.91[j]
Isomer **4a**									
I	OH	$[Bu_4N][PF_6]$	−0.78(99)	1.25	Not observed	—	—	+1.20[g] (130)	+0.73
Isomer **4b**									
I	OH	$[Bu_4N][PF_6]$	−0.83[g] (174)	−1.30	Not observed	—	—	+0.97[e] (360)	+0.51
Isomer **8a**									
I	NHMe	$[Bu_4N][PF_6]$	−1.16[e,h]	−1.63	Not observed	—	—	+0.98(79)	+0.47

[a] First reduction wave, in V ($\Delta E = E_p^a - E_p^c$, in mV); scan speed 50 mV s^{-1}. [b] *vs.* ferrocene–ferrocenium couple ($\Delta E_p = E_p^a - E_p^c = 80$–120 mV). [c] Second reduction wave; scan speed 50 mV s^{-1}. [d] In mV. [e] Irreversible. [f] Anodic peak; very weak cathodic peak observed at +1.08 V. [g] Quasi-reversible, $i_c < i_a$ (for reduction potentials) or $i_a < i_c$ (for oxidation processes). [h] E_p^c, no anodic peak. [i] Estimated based on difference between cathodic peaks.

unusual since such methyl signals normally occur in the region δ 2–3. From the detailed crystal and molecular structures of [{Mo(NO)[HB(dmpz)$_3$]I}$_2$O] (Fig. 1), it is clear that two of the pyrazolyl rings in adjacent HB(dmpz)$_3$ ligands are face-to-face and it may be presumed that the asymmetrically-substituted species described here, having been derived from rotamer **B** of this iodide, will have similar conformations, and so ring current shielding must be responsible for the extension of methyl proton chemical shifts to such high fields. However, it is not possible to determine the precise molecular structures of the new binuclear species solely on the basis of their ^{1}H NMR spectra.

It is evident from the NMR spectra of the isomers of **4**, **8** and **9** that significant differences exist between the sets of signals derived from the pyrazolyl protons. However, the most obvious spectral differences appear in proton chemical shifts of *other* groups attached to the metal, *e.g.* OH, OMe, OEt or OCOMe. Thus, in the asymmetric monohydroxo species **4a** and **4b** the hydroxyl proton signal in one isomer occurs at δ 9.36 and at 9.40 in the other. Only one isomer of **5** has been isolated, with δ_{OCH_3} 5.04, whereas in **8** NH proton signal occurs at δ 10.54 in isomer **8a** and 9.55 in isomer **8b**, whereas the methylamide methyl proton signals occur at δ 4.52 in **8a** and 4.25 in **8b**; differences of 0.99 and 0.27 ppm, respectively. Similar observations can be made in the spectra of **9**, the differences between the pairs of NH, CH_2 and CH_3 proton signals being 1.04, 0.22 and 0.37 ppm, respectively. In the symmetrically-substituted **6**, **7** and **1**, differences between the chemical shifts of the protons in each X are also detectable; 0.35 ppm when X = OMe (**6**), 0.46 (CH_2) and 0.35 (CH_3) ppm when X = OEt (**7**), but only 0.01 ppm when X = OCOMe (**1**).

It should be noted that the protons attached to the C atom α to the O or NH groups bonded to each Mo atom resonate at relatively low fields. This effect is well established,[10] being due to the strong electronegativity of the [Mo(NO){HB(dmpz)$_3$}X]$^+$ group.

Electrochemical studies

The cyclic voltammetric behaviour of the binuclear compounds [{Mo(NO)[HB(dmpz)$_3$]X}$_2$O] (X = OH, OCOPh or OMe) at a bead electrode in dichloromethane, using either $[NBu_4][PF_6]$ or $[NBu_4][BF_4]$ as base electrolyte, are recorded in Table 2.

From our previous studies of [{Mo(NO)[HB(dmpz)$_3$]X}$_2$O] (X = Cl or I) we would expect the dinuclear species here to exhibit two reduction processes corresponding to formation of [{Mo(NO)[HB(dmpz)$_3$]X}$_2$O]$^{-,2-}$. However, we were unable to detect this second reduction in **3** and **6**, presumably because the reduction wave occurs within or at potentials more anodic than the decomposition of the medium (*ca.* −2.10 V *vs.* SCE). Although the first reduction process in the species with **3** and **6** is irreversible, making comparison of E_f values somewhat speculative, the value of E_f^1 becomes more negative in the order X = I ≤ Cl < OCOPh < OH < OMe in [{Mo(NO)[HB(dmpz)$_3$]X}$_2$O], which broadly follows that expected from the electrochemical behaviour of [Mo(NO){HB(dmpz)$_3$}XY].[11] The first reduction process in **2** is apparently reversible, and although we did not determine the number of electrons transferred in this particular electrode reaction directly by coulometry, by comparison with our earlier work[2] it is very likely that one electron is involved. Although we were only able to detect the cathodic peak E_p^c of the second reduction process of **2**, due to generation of [{Mo(NO)[HB(dmpz)$_3$](OCOPh)}$_2$O]$^{2-}$, we have estimated ΔE_f (here being $E_p^{c1} - E_p^{c2}$) to be 1240 mV, indicating a substantial interaction between the two metal-based redox centres, consistent with our findings from the electrochemical behaviour of [{Mo(NO)[HB(dmpz)$_3$]X}$_2$O] (X = Cl or I).[1]

The electron-transfer characteristics of **4a** and **4b** are significantly different. This suggests that these two compounds are isomers rather than enantiomers since we would expect the electrode behaviour of enantiomers to be virtually identical, assuming that the electrode has no chiral properties. Reduction of **4a** is more anodic (*ca.* 200 mV) than that of the symmetrical **3** which is consistent with the electronegativity of I *versus* OH. The formation potential for [**8a**]$^-$ was significantly more cathodic than that for [**4**]$^-$ which is also consistent with electronegativity effects.

We also observe an irreversible cathodic electron transfer in all three compounds investigated, in the range 0.97–1.40 V, perhaps due to the formation of unstable [{Mo(NO)[HB(dmpz)$_3$]X}$_2$O]$^+$. Although similar behaviour was detected in the chloro and iodo μ-oxo species, we have rarely detected cathodic electrode processes in species of the type [Mo(NO){HB(dmpz)$_3$}XY] (X, Y are anionic ligands), and the formation potentials are too cathodic for convenient synthesis.

Reduction of [{Mo(NO)[HB(dmpz)$_3$](OCOPh)}$_2$O] and EPR spectral characterisation of the product. The first reduction potential of the benzoate **2** is such that its reduction to [{Mo(NO)[HB(dmpz)$_3$](OCOPh)}$_2$O]$^-$ was easily achieved using cobaltocene. Preliminary EPR spectral studies of the monoanion so formed in toluene reveals that it has features very similar to those of [{Mo(NO)[HB(dmpz)$_3$]Cl}$_2$O]$^-$.[1] Thus there is a signal at $g_{iso} = 1.9790$ and $A_{Mo} = 5.0$ mT, consistent

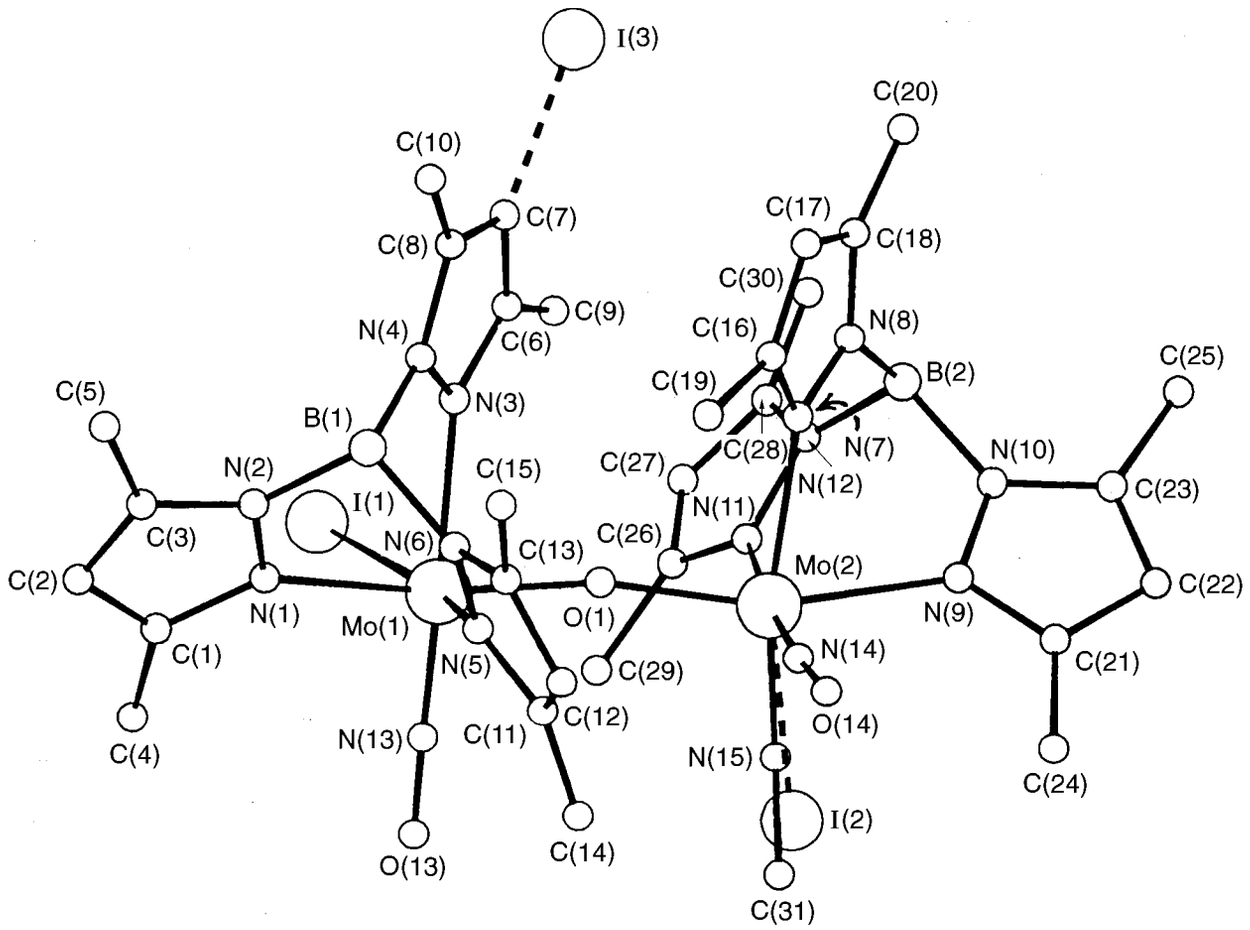

Fig. 2 A general view of the structure of the dinuclear complex [I{HB(dmpz)$_3$}(NO)MoOMo(NO){HB(dmpz)$_3$}(NHMe)] **8a**, showing the atom numbering (the hydrogen atoms are omitted for clarity). The dotted lines represent bonds with partially occupied iodide ligands

with a single electron coupled to a molybdenum nucleus [sextet, ^{95}Mo (15.72%) and ^{97}Mo (9.46%), $I = \frac{5}{2}$]. This gradually broadens as the temperature of the solution is raised from room temperature, disappearing altogether by the time the temperature reached 320 K. The spectral behaviour is reversible, the sextet structure reappearing on cooling to room temperature. This behaviour is being further investigated, but it seems likely that the mixed-valence species [{Mo(NO)[HB(dmpz)$_3$](OCOPh}$_2$O]$^-$ is valence-trapped at or below room temperature, perhaps starting to exhibit electron exchange behaviour (inter- or intramolecular) as the temperature increases. This conclusion is generally consistent with the behaviour of [{Mo(NO)[HB(dmpz)$_3$]X}$_2$O]$^-$ (X = Cl or I) where we have suggested that the redox orbitals on the metal centres (d_{xy}, assuming the Mo–N–O bond defines the *z* axis) are mutually orthogonal because of the structural relationships of the two {Mo(NO)[HB(dmpz)$_3$]X} fragments and delocalisation over the Mo–O–Mo group is impossible.[1,12]

Structural studies

The material crystallographically examined is actually a mixture of three compounds, the major (90%) component of which is **8a**. The second component is the known [{Mo(NO)[HB(dmpz)$_3$]I}$_2$O] whose structure is that of enantiomer **B** in Fig. 1. This structure bears a very close relationship to that of **8a**, where the NHMe group may be notionally interchanged with one I atom. The third, very minor fraction, is a compound in which the hydrogen of one pyrazolyl ring has been partially substituted by an iodine atom, although it does not seem to affect the overall geometry of the complex.

The nature of the isomer **8a** was established unequivocally by the crystal structure study. A general view of the complex is shown in Fig. 2, which also indicates the atom numbering

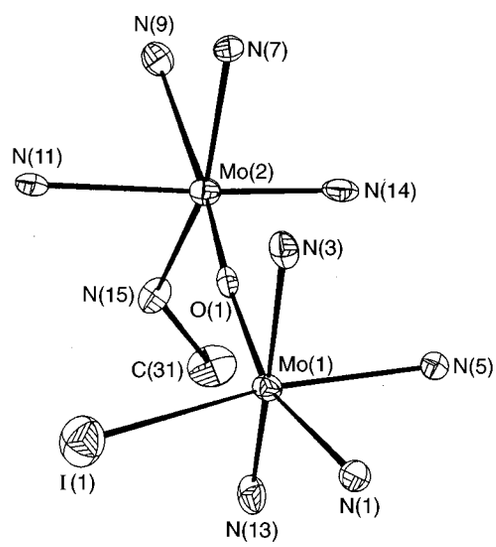

Fig. 3 Illustration of the dinuclear core in the structure of [I{HB(dmpz)$_3$}(NO)MoOMo(NO){HB(dmpz)$_3$}(NHMe)] **8a**

scheme used, the stereochemistry of the binuclear core being shown more clearly in Fig. 3. An important aspect of the present structural determination is that it represents authentication of an oxo-bridged asymmetrically-substituted binuclear complex, [X{HB(dmpz)$_3$}(NO)MoOMo(NO){HB(dmpz)$_3$}Y], where the X and Y ligands are different (X = I, Y = NHMe).

The basic geometry of the dinuclear complex **8a** is constructed from two distorted octahedra sharing a corner occupied by the bridging oxo group and having an eclipsed configuration. The N (dmpz)–Mo–N (dmpz) angles, determined by the stereochemistry of the HB(dmpz)$_3$ ligand, are all

acute [75.3(3)–87.3(3)°]. Distortions from octahedral geometry are also reflected in other angles involving the *cis* atoms [85.2(3)–106.9(3)°] as well as those involving the *trans* atoms [160.9(2)–178.4(3)°]. Similar distortions from ideal octahedral geometry were also observed in the pair of enantiomers reported earlier and are a common feature of this class of compounds. The Mo–O (bridge) distances [1.884(6) and 1.948(6) Å] are significantly different, which indicates a slight asymmetry in the Mo–O–Mo bridge. The bridge angle [167.8(4)°] is also significantly non-linear. The average value of the Mo–O (bridge) bonds (1.916 Å) is very close to those in the two enantiomers of [{Mo(NO)[HB(dmpz)$_3$]I}$_2$O] (1.895, 1.910 Å), and is consistent with significant Mo–O d_π–p_π bonding.[1,10,13] The Mo–I [2.768(1) Å (ignoring the partially occupied I)], Mo–N (NO) [1.752(9), 1.773(9) Å] and N–O bond lengths [1.205(10), 1.207(10) Å], and the Mo–N–O bond angles [175.2(7), 176.1(8)°] are also similar to the corresponding values in the rotamers of [{Mo(NO)[HB(dmpz)$_3$]I}$_2$O]. The dimensions of the HB(dmpz)$_3$ ligands are as expected [B–N = 1.52(2)–1.57(1) Å, N–B–N angles 107.0(8)–110.7(7)°], and their relative dispositions around the Mo atoms are determined by inter-ligand steric interactions which result in a rigid interlocking system. Two dmpz moieties [N(3),N(4),C(6)–C(10) and N(7),N(8),C(16)–C(20)] from two different ligands approach each other quite closely with several non-hydrogen contacts less than 3.5 Å [C(6)···C(16) 3.278, N(3)···C(19) 3.342, C(9)···N(8) 3.431, C(7)···C(1) 3.444 Å]; these two rings are also nearly parallel to each other (dihedral angle 3.0°). The dihedral angles between the five-membered rings in the HB(dmpz)$_3$ ligands bonded to Mo(1) and Mo(2) are 110.3, 120.1, 129.6 and 106.9, 126.0, 126.5°, respectively, the larger of these values being explained by the 'embrace' of the oxo and I/NHMe groups by the given pair of rings.

In principle, 16 isomers are possible for [I{HB(dmpz)$_3$}(NO)MoOMo(NO){HB(dmpz)$_3$}(NHMe)], assuming that only eclipsed configurations of the molecule are considered. This arises because there are four rotamers for the molybdenum nitrosyl centre generated by rotation of one of the {Mo(NO)[HB(dmpz)$_3$]X} groups by 90° around the Mo–O–Mo bond axis. Each of the single centres can have either *R* or *S* configuration:‡ the possible types are [*R*-(Mo–I)–*R*-(Mo–NHMe)], [*S*-(Mo–I)–*S*-(Mo–NHMe)], [*R*-(Mo–I)–*S*-(Mo–NHMe)] and [*S*-(Mo–I)–*R*-(Mo–NHMe)] (Figs. 4 and 5). The X-ray analysis undertaken in this study cannot give the absolute configuration at each metal centre, but it is apparent from the structure of **8a** that the metal configurations are *S–S* or *R–R*, *i.e. S–S* **C** in Fig. 4. Of course, this refers to the solid state, and we must assume that the solution from which **8a** was obtained was a racemic mixture and we picked only one enantiomer for crystallographic studies. Having detected significant differences between the physical properties of **8a** and **8b**, we must conclude that **8b** is not the other enantiomer of **8a**. It must therefore be a different isomer (rotamer). Similar remarks must apply to **4a** and **4b** and **9a** and **9b**.

It should be realised that although there must be several possible rotamers for this class of compounds in solution, only a few can be energetically favoured in the solid state because of large inter-ligand steric interactions. To determine the most energetically favoured orientations about the metal centres, we undertook a conformational analysis of **8** using the molecular modelling package CHEM-X.[14] Using atomic coordinates the Mo(1) centre and its associated ligands (including the bridging oxygen) were kept in fixed positions whilst the Mo(2)(NO){HB(dmpz)$_3$}(NHMe) moiety was rotated through 360° and the relative energy calculated at 2° iterations. The reference for rotation was taken as the torsion angle (φ) Mo(2)–O(1)–Mo(1)–I(1). For simplicity of calculations, only the non-hydrogen atoms were included in the model, and the results of this study are shown graphically in Fig. 6. This Figure shows that there are only two energetically favoured conformations which are *ca.* 185° apart in rotation about the Mo(1)–O(1) bond, assuming the relative positions of the NO groups, I and NHMe, which restricts the model to **C** and **D** (and their *R–R* enantiomers) shown in Fig. 4. One of these positions, with an energy minimum centred at 51° (E_1), is quite sharp and narrow, whilst the other centred at −130° (E_2) has a very large, broad and nearly flat energy minimum ranging from *ca.* −150 to −110°. The former position corresponds to a very rigid interlocking framework, *viz.* **D** in Fig. 4; the latter, in contrast, reflects about 20° of rotational flexibility on either side of the centre *viz.* **C** in Fig. 4. The first minimum corresponds to an eclipsed configuration of the two octahedra, while the position, size and shape of the second minimum suggests enough of a degree of orientational freedom to allow the complex to adopt any configuration from preferably eclipsed (−130°) to partially

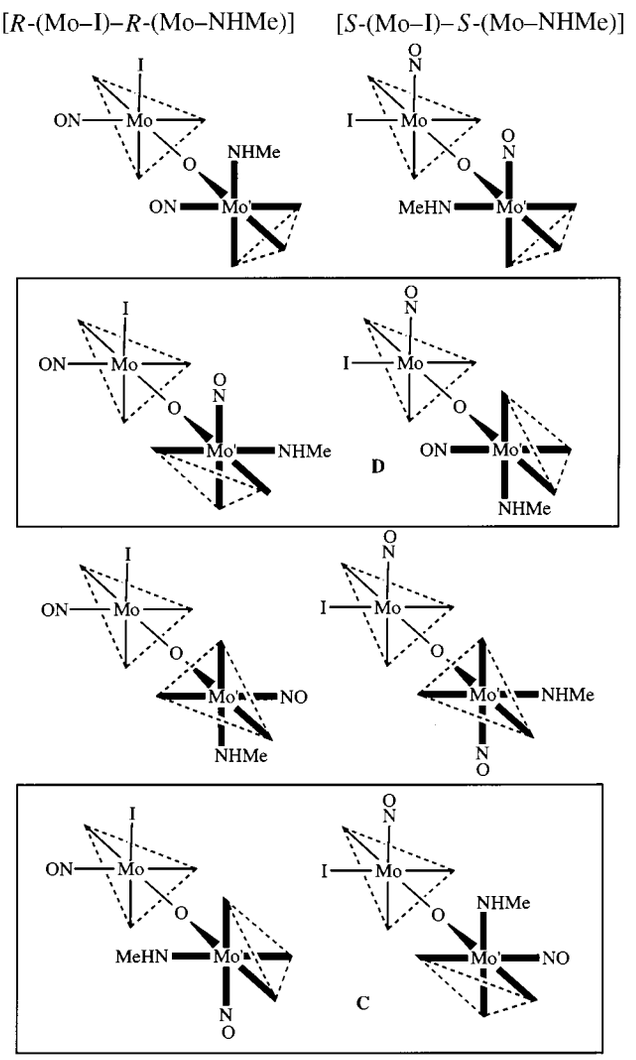

Fig. 4 Possible structures for **8** as *R–R*/*S–S* pairs of enantiomers: **8a** identified as enantiomeric pair **C**

‡ Following Cahn–Ingold–Prelog rules, the relative configurations of the metal fragments defined as {Mo(NO)[HB(dmpz)$_3$](O)} and {Mo(NO)[HB(dmpz)$_3$](NHMe)(O)} are as shown:

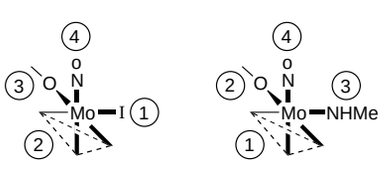

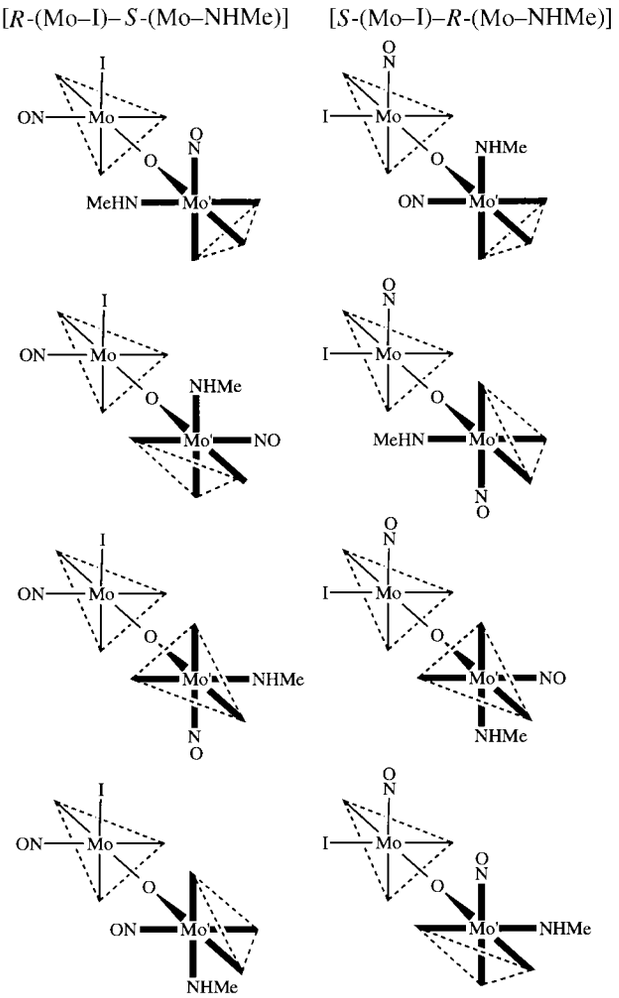

Fig. 5 Possible structures for **8** as *R–S*/*S–R* pairs of enantiomers

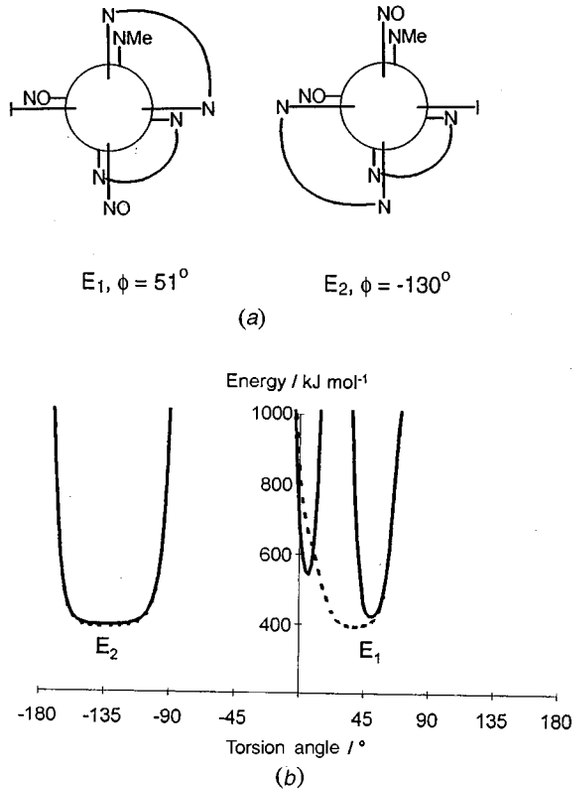

Fig. 6 (*a*) Newman projections along the Mo–O–Mo axis of the dinuclear core showing the two eclipsed conformations (E_1 and E_2) of [I{HB(dmpz)$_3$}(ON)MoOMo(NO){HB(dmpz)$_3$}(NHMe)]. The third Mo–N bond involving the HB(dmpz)$_3$ ligand, not shown in the figure, lies normal to the plane of the paper. (*b*) Graphical representations of the energy minima showing the two possible conformations for [I{HB(dmpz)$_3$}(NO)MoOMo(NO){HB(dmpz)$_3$}(NHMe)] (solid lines) and the corresponding iodide [{Mo(NO)[HB(dmpz)$_3$]I}$_2$O] (the torsion angle φ is defined in the text)

staggered (closer to −110 and −150°). The energies for strictly staggered configurations are extremely high, and so these arrangements are ruled out. This study therefore suggests that of several possible conformers in solution, only two, both eclipsed, should be stable and isolable in the solid state. The actual structure of **8a** (*S–S* **C** in Fig. 4) corresponds to the energy position E_2[φ(observed) = 135°] in Fig. 6, and represents the energetically most favoured conformer with steric interactions involving only the dmpz rings (see above) and none with the methylamino group. The conformer corresponding to the narrower E_1 position (*S–S* **D** in Fig. 4) on the other hand represents a structure with interactions involving both the dmpz and the methylamino ligands, and therefore it would be less favourable than that actually observed.

When the methylamino group on Mo(2) is substituted by an iodine (minor component of the structure), the position, shape and size of E_2 remains virtually unaltered, but E_1 becomes bigger and broader (centre shifted to *ca.* 35°), and in this case both conformations (**A** and **B** in Fig. 1) appear to be equally favourable. This is borne out by our isolation of the two rotamers of [{Mo(NO)[HB(dmpz)$_3$]I}$_2$O].[1,4] From the simple studies of space-filling models and from the molecular mechanics calculations, it seems very unlikely that other rotamers/isomers with different arrangements of the NO, halide and/or other substituents will be stable.

Conclusion

We know that the precursor to all the substitutions in this work, [{Mo(NO)[HB(dmpz)$_3$]I}$_2$O], has structure **B**[1] with *R–S* configuration at the metal centres, and we have shown that one of the substituted derivatives, **8a**, has a closely related structure with *S–S* (or *R–R*) configuration. Interconversion of **8a** into **8b** in solution was *not* observed, but we believe that **8b** is a rotamer rather than the enantiomer of **8a**. Of course, we do not know the intimate mechanism for the formation of these compounds, but from an inspection of molecular models of this group of compounds there appears to be no obvious steric preference for the site of attack by NH_2Me on [{Mo(NO)[HB(dmpz)$_3$]I}$_2$O], so that generation of isomers is very reasonable. The same applies to **9a** and **9b**. Thus, we may speculate on the nature of **8a** and **8b** in terms of the substitution of I by NHMe at Mo or Mo′ (labelling as shown in Fig. 1). If the I atom on Mo is substituted, the *S–S* enantiomer of **C** is formed (Fig. 7), but if displacement occurs at Mo′, the *R–R* enantiomer of **D** is generated. These two structures are entirely consistent with the results of our conformation analysis described above.

So in response to the issues raised in the introduction we may conclude (*a*) that substitution at the Mo–O–Mo centre can proceed in steps, and (*b*) that there are close structural relationships between the precursor and the product and only two isomers are apparently formed (as enantiomeric pairs in solution, presumably). Rotation about the Mo–O–Mo bond system does not appear to occur during the substitution but we are unable to draw any more specific conclusions about the mechanism.

In the structural analysis of **8a** the occurrence of the ring-iodinated species [I{HB(dmpz)$_2$(4-I-dmpz)}(NO)MoOMo(NO){HB(dmpz)$_3$}I] was a surprise. Halogenation of pyrazolyl rings in tris(pyrazolyl)borate metal chemistry is not unprecedented, direct chlorination and bromination of [Mo(CO)$_2$(NO){HB(dmpz)$_3$}] affording [Mo(NO){HB(4-Cl-dmpz)$_3$}Cl$_2$] and [Mo(NO){HB(dmpz)$_{3-n}$(4-Br-dmpz)$_n$}Br$_2$].[10] The related [W(NO){HB(4-Br-dmpz)(dmpz)$_2$}Br$_2$] and [Re-

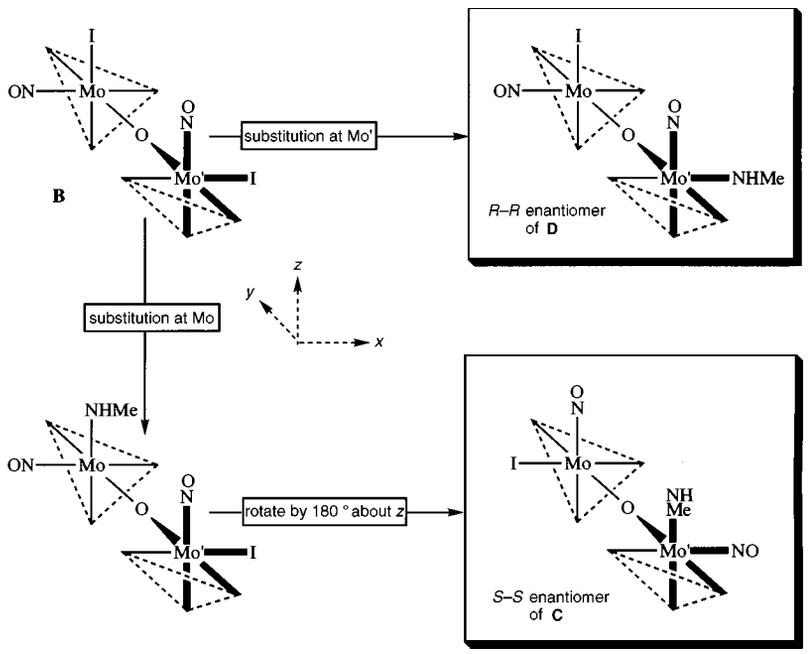

Fig. 7 Postulated structural relationships between $[\{Mo(NO)[HB(dmpz)_3]I\}_2O]$, **B** and $[I\{HB(dmpz)_3\}(NO)MoOMo(NO)\{HB(dmpz)_3\}(NHMe)]$ **8a** and **8b**

$(CO)_3\{HB(4\text{-}X\text{-}dmpz)_3\}]$ are formed similarly.[15] It is for this reason that we prefer to generate chloro and bromo molybdenum nitrosyls from the diiodide $[\{Mo(NO)[HB(dmpz)_3]\}I_2]$, prepared *in situ*, by its treatment with benzyl chloride or bromide. Prior to this work, we had never observed iodination of pyrazolyl rings, which we presume must occur *via* radical reactions.

The dimethylamine solvate in the material examined crystallographically must presumably arise from impurity in the gaseous NH_2Me used in the preparation of **8**. However, no conclusive spectroscopic evidence could be obtained for its presence in the purified isomers of **8**, although there are weak ^1H NMR data obtained from solutions of NH_2Me which appear to be consistent with $NHMe_2$.

The EPR spectral behaviour of the mono-reduced species $[\{Mo(NO)[HB(dmpz)_3](OCOPh)\}_2O]^-$ is similar to that of $[\{Mo(NO)[HB(dmpz)_3]X\}_2O]^-$ (X = Cl or I), and while the benzoate has not yet been examined in detail, it conforms to the general pattern of Class I valence-trapped behaviour in these compounds at room temperature. Clearly, more detailed spectroscopic studies, particularly of the behaviour of the EPR spectra with variations in temperature, are warranted.

Acknowledgements

We wish to thank Professor J. A. McCleverty and the School of Chemistry, University of Bristol, for provision of facilities to carry out some experiments, and for much discussion of the results. We would like also to acknowledge particularly the valuable comments made by Dr. S. S. Kurek concerning rotameric and enantiomeric relationships in the class of compounds described here. We are grateful to the SERC/EPSRC for support of this work through a studentship (to S. J. C.) and for the provision of the SERC X-Ray Crystallographic Service at Cardiff and the EPR instrumentation at Bristol, and to the Politechnika Krakowska for leave of absence (to A. W.).

References

1 A. Wlodarczyk, J. P. Mayer, S. Coles, D. E. Hibbs, M. H. B. Hursthouse and K. M. A. Malik, *J. Chem. Soc., Dalton Trans.*, 1997, 2597.
2 S. L. W. McWhinnie, S. M. Charsley, C. J. Jones, J. A. McCleverty and L. J. Yellowlees, *J. Chem. Soc., Dalton Trans.*, 1993, 413.
3 H. Adams, N. A. Bailey, G. Denti, J. A. McCleverty, J. M. A. Smith and A. Wlodarczyk, *J. Chem. Soc., Dalton Trans.*, 1983, 2287.
4 C.-Y. Cheng, C. E. Johnson, T. G. Richmond, Y.-T. Chen, W. C. Trogler and F. Basolo, *Inorg. Chem.*, 1981, **20**, 3167; B. F. G. Johnson, B. L. Haymore and J. R. Dilworth, *Comprehensive Coordination Chemistry*, eds. G. Wilkinson, R. G. Gillard and J. A. McCleverty, Pergamon Press, Oxford, 1987, ch. 13, p. 99.
5 J. A. Darr, S. R. Drake, M. B. Hursthouse and K. M. A. Malik, *Inorg. Chem.*, 1993, **32**, 5704.
6 N. P. C. Walker and D. Stuart, *Acta Crystallogr., Sect. A*, 1983, **39**, 158; adapted for FAST geometry by A. I. Karaulov, University of Wales Cardiff, 1991.
7 G. M. Sheldrick, *Acta Crystallogr., Sect. A*, 1990, **46**, 467.
8 G. M. Sheldrick, SHELXL 93, Program for Crystal Structure Refinement, University of Göttingen, 1993.
9 K. Davies, SNOOPI, Program for Crystal Structure Drawing, University of Oxford, 1983.
10 J. A. McCleverty, D. Seddon, N. A. Bailey and N. W. Walker, *J. Chem. Soc., Dalton Trans.*, 1976, 898.
11 C. J. Jones, J. A. McCleverty, B. D. Neaves, S. J. Reynolds, H. Adams, N. A. Bailey and G. Denti, *J. Chem. Soc., Dalton Trans.*, 1986, 733; N. Al Obaidi, M. Chaudhury, D. Clague, C. J. Jones, J. C. Pearson, J. A. McCleverty and S. S. Salam, *J. Chem. Soc., Dalton Trans.*, 1987, 1733.
12 J. Boinvoisin and J.-P. Launay, unpublished work.
13 J. A. McCleverty, A. E. Rae, I. Wolochowicz, N. A. Bailey and J. M. A. Smith, *J. Chem. Soc., Dalton Trans.*, 1982, 951.
14 E. K. Davies, CHEM-X, Program for Molecular Modelling, Chemical Design Ltd., Oxford, 1994.
15 J. A. McCleverty, A. E. Rae, I. Wolochowicz, N. A. Bailey and J. M. A. Smith, *J. Chem. Soc., Dalton Trans.*, 1982, 420; J. A. McCleverty and I. Wolochowicz, *J. Organomet. Chem.*, 1979, **169**, 289.

Received 1st *September* 1996; *Paper* 7/04179I